Applied Catalysis B: Environmental 125 (2012) 21–27

Contents lists available at SciVerse ScienceDirect

Applied Catalysis B: Environmental

journal homepage: www.elsevier.com/locate/apcatb

The effect of TiO_2 doping on the catalytic properties of nano-Pd/SnO_2 catalysts during the reduction of nitrate

Yan-ni Guo[a,1], Jian-hua Cheng[a,2], Yong-you Hu[a,b,*], De-hao Li[c,3]

[a] Ministry of Education Key Laboratory of Pollution Control and Ecological Remediation for Industrial Agglomeration Area, College of Environmental Science and Engineering, South China University of Technology, Guangzhou 510006, China
[b] State Key Lab of Pulp and Paper Engineering, College of Light Industry and Food Science, South China University of Technology, Guangzhou 510640, China
[c] School of Chemical & Environmental Engineering, Guangdong University of Petrochemical Technology, Maoming 525000, China

ARTICLE INFO

Article history:
Received 17 March 2012
Received in revised form 7 May 2012
Accepted 9 May 2012
Available online 17 May 2012

Keywords:
Palladium
Titanium dioxide
Tin dioxide
Nitrate
Catalytic reduction

ABSTRACT

The monometallic catalysts $Pd/TiO_2–SnO_2$ and Pd/SnO_2 prepared by impregnation method were investigated for their ability to catalyze the reduction of nitrate with formic acid as the reducing agent and were characterized by X-ray diffraction (XRD), BET surface area, transmission electron microscopy (TEM) and X-ray photoelectron spectroscopy (XPS). Pd and TiO_2 were in high dispersion on the surface of the SnO_2 support when the mol fraction of TiO_2 was less than 15%. The SnO_2 crystal lattice was partially replaced by titanium ions, causing SnO_2 lattice distortion and resulting in the increase of oxygen vacancies as catalytic active sites. The best catalytic properties of the formic acid–$Pd/TiO_2–SnO_2$ system were achieved at a mol fraction of 10% TiO_2. Compared with the Pd/SnO_2 catalyst, the catalytic activity of $Pd/TiO_2–SnO_2$ increased by 48% from 2.08 mg/(min g_{cata}) to 4.00 mg/(min g_{cata}), while the NH_4^+ concentration decreased from 13.0 mg/L to 5.2 mg/L. The catalytic activity, selectivity and stability of the $Pd/TiO_2–SnO_2$ catalyst were superior to those of Pd/SnO_2 with the same Pd loading and formic acid concentration. The results of the XPS analysis indicated that the catalysts Pd/SnO_2 and $Pd/TiO_2–SnO_2$ were of high oxygen vacancy. $Pd/TiO_2–SnO_2$ has better catalytic properties than Pd/SnO_2 may attribute to the increased amount of oxygen vacancy after TiO_2 doping.

1. Introduction

Nitrate is becoming one of the most ubiquitous pollutants in many countries due to rapid growth in both agricultural and industrial activities [1]. High concentrations of nitrate in the water are harmful because they reduce to nitrites, which can cause blue baby syndrome and cancer [2]. Therefore, methods for treating nitrate contamination are both urgent and essential. Chemical catalytic reduction is considered one of the most promising methods due to its ability to effectively and thoroughly remove nitrate [3]. The catalytic reduction of nitrate using hydrogen over solid catalysts was first demonstrated by Tacke and Vorlop [4]. Their experimental results proved that it is necessary to activate the precious metal by an additional promoter to reduce nitrate. The promoters they focused on were Cu, Sn and In [5–9]. However, these bimetallic catalysts have insufficient activity and selectivity for practical usage. Previous research indicates that the molar ratio between Pd and the promoter significantly impacts the catalytic activity and selectivity. Therefore, the proper amount of the promoter was difficult to determine [10–13]. For this reason, monometallic catalysts without a promoter are desirable.

Previous studies demonstrated that monometallic catalysts, such as Pd/Al_2O_3, are inactive for nitrate reduction. However, recent studies involving monometallic catalysts without an additional promoter have been reported based on the idea that nitrate reduction could be catalyzed by a catalyst containing a noble metal to chemisorb hydrogen and a support with redox properties [14–16]. Epron et al. used a rare earth oxide CeO_2 as an active support for Pd/CeO_2 catalysts, resulting in a high activity (33 mmol/(min g_{cata})) in reducing nitrates but a poor selectivity to nitrogen (NH_4^+ was 80% of the product) [15]. Gavagnin et al. found that the monometallic catalyst Pd/SnO_2, which used the semiconductor SnO_2 as a carrier for the reduction of nitrates, also showed high catalytic activity and selectivity compared with bimetallic catalysts under the same conditions [16]. The reaction mechanisms suggested that the oxygen vacancies were involved as active sites for reducing nitrates. If

* Corresponding author at: College of Environmental Science and Engineering, South China University of Technology, Guangzhou, 510006, China.
Tel.: +86 20 39380506; fax: +86 20 39380508.
E-mail addresses: gynhz@126.com (Y.-n. Guo), jhcheng@scut.edu.cn (J.-h. Cheng), ppyyhu@scut.edu.cn, hidden_heart19800129@yahoo.com.cn (Y.-y. Hu), dehlee@163.com (D.-h. Li).
[1] Tel.: +86 13401016836.
[2] Tel.: +86 13926448812.
[3] Tel.: +86 13580026968.

0926-3373/$ – see front matter © 2012 Elsevier B.V. All rights reserved.
http://dx.doi.org/10.1016/j.apcatb.2012.05.012

the monometallic catalyst Pd/SnO_2 can show high catalytic activity and selectivity compared to bimetallic catalysts, it could positively affect the development of catalytic reduction nitrate technology.

Furthermore, due to the high surface area and homogeneity characteristics of nanometer-scale materials, nano-Pd/SnO_2 catalysts will be the main focus of development. Wu et al. prepared nano-Pd/SnO_2 catalysts with high activity and selectivity using thermal decomposition, but the conglomeration phenomenon decreased the catalytic activity and selectivity of the catalyst due to the small nanometer particle size. A common method to reduce the conglomeration phenomenon is doping. Liu et al. found that semiconductor materials SnO_2 doped with TiO_2 could reduce the conglomeration phenomenon of pure SnO_2 and create more oxygen vacancies because of the interaction between SnO_2 and TiO_2 [17].

Thus, the composite semiconductor materials TiO_2–SnO_2 may be more appropriate than SnO_2 to be used as nitrate reducing carrier. However, the use of the composite oxide TiO_2–SnO_2 has never been reported as a support. In this study, the monometallic catalysts Pd/SnO_2 and Pd/TiO_2–SnO_2 were prepared using the impregnation method and were characterized by X-ray diffraction (XRD), BET surface area, transmission electron microscopy (TEM) and X-ray photoelectron spectroscopy (XPS).

The catalytic properties of Pd/SnO_2 and Pd/TiO_2–SnO_2 were compared with different doping TiO_2 contents, Pd loadings and formic acid concentrations. The main objective of this work was to further verify the oxygen vacancies mechanism of monometallic catalysts and to show possible ways to improve the catalytic activity and selectivity.

2. Materials and methods

2.1. Catalyst preparation

TiO_2–SnO_2 supports were prepared by the precipitation method [17]. Briefly, a solution of 0.5 mol/L $Ti(SO_4)_2$ and $SnCl_4{\cdot}5H_2O$ was prepared according to a certain molar ratio and was dripped with the mixed water solution and ammonia into an alkaline buffer solution ($NH_3{\cdot}H_2O/NH_4Cl$ at pH 8). The buffer solution was stirred vigorously and maintained at pH 8 during the titration process. The precipitate was incubated for 2 h at room temperature, filtered, washed 5 times with deionized water, dried at 120 °C for 12 h, and finally calcinated in air at 500 °C for 4 h.

The metal precursors $PdCl_2$ with Pd loading of 2–6 wt% were dripped into 5 mL deionized water with 1–2 drops of hydrochloric acid. Two grams of TiO_2–SnO_2 carriers were added to this aqueous solution at room temperature while being stirred periodically. The above mixed solution was dried at 100 °C for 16 h, burnt in air at 350 °C for 2 h, reduced in sodium borohydride ($NaBH_4$) solution at room temperature, washed 5 times with deionized water, and finally dried in a vacuum oven to form the monometallic catalysts Pd/TiO_2–SnO_2.

2.2. Catalyst characterization

The X-ray diffraction (XRD) patterns were obtained by a Bruker D8 X-ray diffraction meter equipped with a Ni-filtered Cu Kα radiation (λ = 1.54056 nm). The scanning rate was 10/min in the 2θ diffraction angle between 10° and 80°. The SnO_2 particle size was calculated based on the SnO_2 (1 1 1) diffraction peak.

The BET specific surface areas were measured by nitrogen adsorption and desorption at −196 °C on a Micromeritics ASAP 2000 instrument. Samples were pre-treated at 200 °C under vacuum (1.33 Pa).

The morphology of the samples was determined by a TEM-3700N with an accelerating voltage of 200 kV. The samples were first suspended in 2-propanol, and then a small drop of each suspension was deposited on a thin amorphous carbon-coated copper grid.

The X-ray photoelectron spectroscopy (XPS) measurements were performed on a VG Escalab X-ray Photoelectron Spectrometer VGX900 using Al Kα radiation. The operating pressure was $<1 \times 10^8$ mbar. In order to prevent the samples to be contaminated by various types of hydrocarbon, oxides and water on the film surface because the samples had to be exposed to the air before XPS analyses, we cleaned film surfaces by argon ion bombardment at the energy of 3 keV for 10 s preceding to each narrow scanning in order to remove the adsorbed species and oxidized layer. The reported binding energies (BEs) were corrected for sample charging by attributing a BE value of 285 eV to the C 1s line.

2.3. Catalytic experiments

Catalytic experiments were performed according to the following procedures: powder catalysts (100 mg) were placed in a three-mouth flask (500 mL). Several ports were installed in the batch reactor, which is convenient for adding formic acid, N_2 and the sample. The wastewater sample (200 mL), which contained 100 mg/L of nitrate, was prepared by dissolving $NaNO_3$ in deionized water. Formic acid (4–24 mmol/L) was then added into the reactor for testing. A magnetic stirrer was used to further mix the liquid. The reaction was maintained at atmospheric pressure and room temperature. Samples were taken from the reactor at 10 min intervals and were filtered through a 0.22 μm membrane. NO_3^- and NO_2^- were determined by a Dionex-90 ion chromatograph, while the NH_4^+–N was determined by using Nessler's method.

The catalytic activity of the catalysts represents the nitrate conversion per unit time and unit quantity of catalysts. The catalytic selectivity represents the amount of NH_4^+ produced during the reaction process such that more NH_4^+ being produced indicated worse selectivity of the catalysts.

3. Results and discussion

3.1. Pd/SnO_2 crystalline phase structure after TiO_2 doping

Fig. 1 shows the XRD spectra of Pd/TiO_2–SnO_2 at different mol fraction of TiO_2. All samples have a tetragonal structure. The characteristic diffraction of Pd and TiO_2 was not observed at TiO_2 mol fraction less than 10%, indicating that Pd and TiO_2 were in high dispersion on the surface of the SnO_2 support or the Pd loading were too low. When the TiO_2 mol fraction exceeded 10%, the characteristic peaks of TiO_2 appeared at the diffraction angle 2θ 48.03° and 75.04°, suggesting that the TiO_2 had exceeded the maximum dispersion content on the surface of SnO_2 and was partly deposited on the surface of SnO_2 in the form of crystalline TiO_2. The emergence of crystalline TiO_2 destroyed the highly decentralized state of TiO_2 on the surface of SnO_2.

Based on the XRD spectra of Pd/SnO_2 and Pd/TiO_2–SnO_2, an increasing amount of TiO_2 caused the intensity of the peaks to weaken and broaden as well as decreased the crystallinity, suggesting that a small part of the tin ions in the SnO_2 lattice were replaced by titanium ions, causing a distorted SnO_2 lattice, reduced crystal symmetry and increased oxygen vacancies [18].

The particle size of Pd/TiO_2–SnO_2 was calculated according to the Scherrer equation $D = k\lambda/(\beta \cos\theta)$ in (Table 1). Moderate amounts of Pd and TiO_2 hinder the SnO_2 from reunification in the nucleation process, and the microporous structures are not damaged, thereby decreasing the sample size and increasing the specific

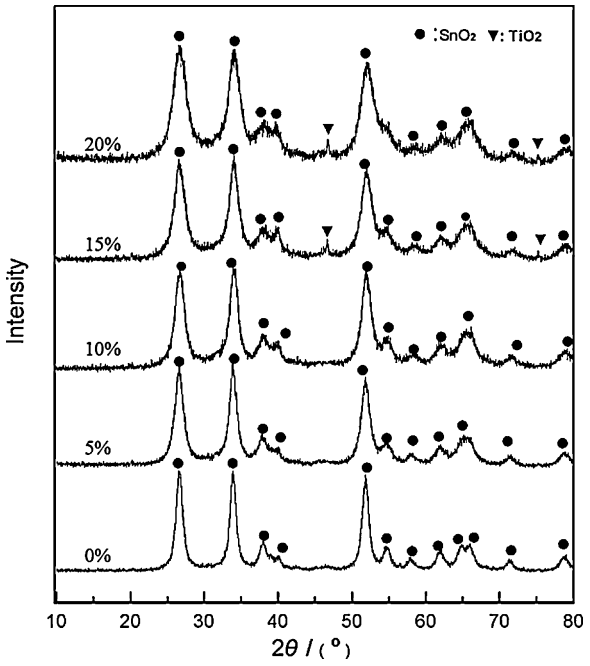

Fig. 1. The XRD patterns of Pd/TiO_2–SnO_2 samples with different TiO_2 mol fraction.

surface area. The XRD spectra showed a formation of TiO_2 crystal phase at TiO_2 mol fraction of 15%, the second phase accelerated the growth of TiO_2–SnO_2 nucleation, increased the particle size of solid materials and decreased the specific surface area. A TiO_2 mol fraction of 10% minimized the catalyst particle's size and maximized its specific surface area. The catalytic reduction of nitrate is a heterogeneous catalysis process in which only the metal atoms on the surface of the catalyst possess catalytic activity, thus, increasing the surface area of the catalyst can improve the catalytic activity [19]. The additional surface area after doping was beneficial to the catalytic activity.

Fig. 2 shows TEM images of the catalyst. Both Pd/SnO_2 and Pd/TiO_2–SnO_2 powder presented a particle size of approximately 10 nm based on the TEM images, which agrees with the XRD results. Based on the TEM images, the Pd/SnO_2 seemed to have serious conglomeration phenomena, but the dispersion of Pd/TiO_2–SnO_2 improved after TiO_2 doping because SnO_2 conglomeration is suppressed by doped TiO_2 to a certain extent. Conglomeration of nano-particles has been deemed as one of the main obstacles in the preparation of nano-materials. The improvement of conglomeration is benefit for the catalytic performance.

3.2. Influence of different TiO_2 mol fraction on the Pd/TiO_2–SnO_2 catalytic properties after TiO_2 doping

Catalytic experiments were investigated at 4% Pd loading, 16.0 mmol/L formic acid and 0–20% TiO_2 mol fraction. Fig. 3 shows the catalytic reduction curves of nitrate at different TiO_2 mol fraction. The catalytic activity here indicated the average rate. The

Table 1
The average particle size and specific surface area of Pd/TiO_2–SnO_2 with different TiO_2 mol fraction.

x (TiO_2) (%)	S_{BET} (m^2/g)	Particle size (nm)
0	59.5	11.7
5	91.5	10.6
10	100.8	9.1
15	98.6	9.5
20	95.3	10.4

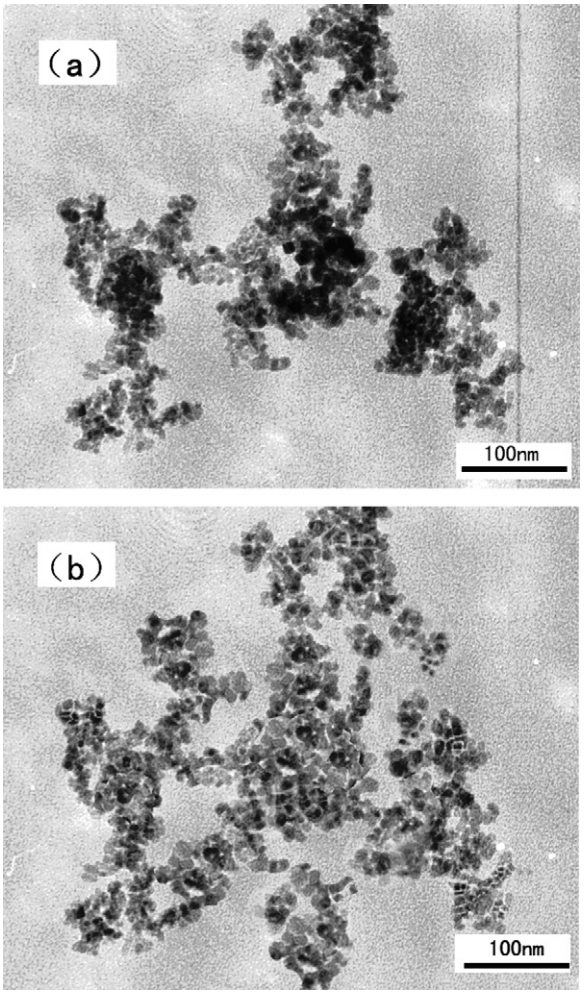

Fig. 2. TEM images of (a) Pd/SnO_2 and (b) Pd/TiO_2–SnO_2.

catalytic activity of the doped Pd/TiO_2–SnO_2 catalysts was higher than that of the simple Pd/SnO_2 catalyst. The best catalytic properties of the formic acid–Pd/TiO_2–SnO_2 system were achieved using a 10% TiO_2 mol fraction, which increased the catalytic activity from 2.08 mg/(min g_{cata}) for Pd/SnO_2 to 4.00 mg/(min g_{cata}) for Pd/TiO_2–SnO_2. Gavagnin et al. gave an view that monometallic catalysts Pd/SnO_2 can catalytic reduce nitrate may rely on the semiconductor properties of SnO_2 [16]. As an effect of the hydrogen

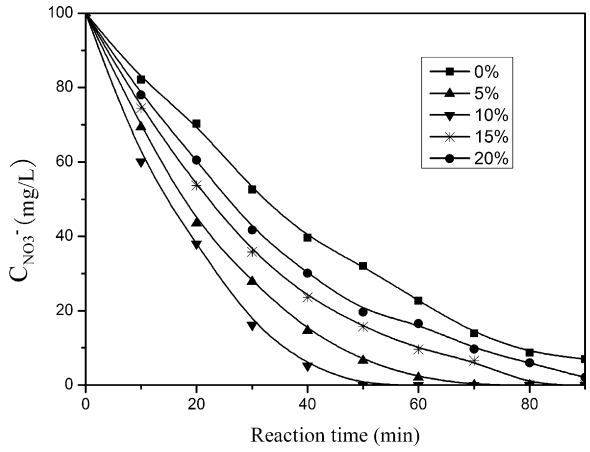

Fig. 3. The catalytic reduction curves of nitrate at different TiO_2 mol fraction.

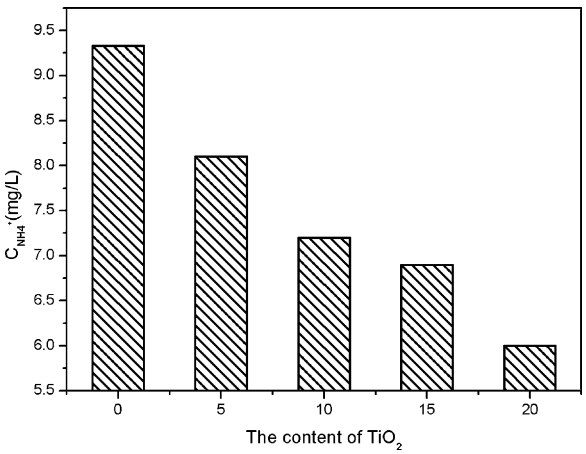

Fig. 4. The influence of different TiO_2 mol fraction on the selectivity of the catalysts.

spill-over from Pd metal, it is conceivable that some oxygen vacancies may be formed on SnO_2 even at room temperature, especially due to the interface between the Pd particles and the support. This reaction would result in the presence of electron-rich Sn centers, which would change the electron density on Pd through a type of ligand effect. Lattice distortion caused by introduced titanium ions could increase the redox active center oxygen vacancies, which may improve the catalytic activity of $Pd/TiO_2–SnO_2$ composite catalysts.

Electrons e^- and vacancies h^+ generated by hydrogen spill-over will conduct electron mobility at the particle interface due to the different conduction band levels for TiO_2 and SnO_2. The migratory process of electrons has two effects on the composite catalysts. On the one hand, this migration can efficiently reduce e^- and h^+ composites, prolonging the service life of the catalysts and improving their catalytic performance; on the other hand, the catalytic activity is related to the conduction band and valence band of the electrode potential. The more positive the valence band of the electrode potential is, the stronger the vacancies' resistance to h^+ oxidation is. Meanwhile, the more negative the conduction band of the electrode potential is, the stronger the reduction potential of the electrons e^- is. The reductive ability of the SnO_2 conduction band is weaker than that of TiO_2, but the oxidation ability of the SnO_2 valence band is stronger than that of the TiO_2 valence band. Therefore, electrons infuse into the conduction band from TiO_2 to SnO_2, and vacancies infuse into the valence band from SnO_2 to TiO_2, leading to a decrease in the h^+ oxidation ability and e^- reductive ability and thereby exerting negative effects on the catalytic activity of $Pd/TiO_2–SnO_2$ composite catalysts. In this experiment, the promoting function dominates when the TiO_2 mol fraction is less than 10%. When the TiO_2 mol fraction increases, the catalytic activity of the catalyst increases. After achieving the optimal proportion of TiO_2, the second aspect of negative gradually strengthened due to the relatively high TiO_2 mol fraction. Therefore, the doped mol fraction of TiO_2 should be controlled at 10% to obtain the best catalytic activity.

Fig. 4 shows the different influence of the TiO_2 mol fraction on the selectivity of the catalysts. The catalytic selectivity was improved by increasing the TiO_2 mol fraction. The NH_4^+ concentration of Pd/SnO_2 was 10.3 mg/L, but $Pd/TiO_2–SnO_2$ was only 5.2 mg/L; thus, the catalytic selectivity of $Pd/TiO_2–SnO_2$ composite catalysts was greatly improved. The NH_4^+ formation is thought to be related to the increase in pH due to the formation of hydroxides during nitrate reduction. Furthermore, a basic pH induces the polarization of the support and has a repulsive effect on nitrates and nitrites, inducing a decrease in the activity and the selectivity to nitrogen [20]. One of the possibilities for green chemical control of the pH is to use a catalyst with an acid–base character. Barrabés et al. modified the acid–base character of the support by introducing several fluoride species into CeO_2 to control the formation of ammonium; as a result, an important decrease in ammonium formation was observed [21]. Previous studies demonstrated that the surface acidity of the composite oxide was higher than that of the single oxide [22]. We have tried to investigate the acid–base character of the support by calculating the pH_{pzc} values for the different samples. The SnO_2 support has a pH_{pzc} of 4.8 and this value decreases to 4.3 for the composite oxide, which demonstrated that the surface acidity of the composite $Pd/TiO_2–SnO_2$ increased by doping with TiO_2. Therefore, the ammonium ion was gradually reduced, and the catalytic selectivity was gradually elevated with an increased amount of TiO_2 doping.

Therefore, 10% TiO_2 mol fraction is suitable for nitrate reduction.

3.3. Influence of different Pd amounts on $Pd/TiO_2–SnO_2$ catalytic properties after TiO_2 doping

Catalytic experiments were investigated using 10% TiO_2 mol fraction, 16.0 mmol/L formic acid and 2–6% Pd loading. Table 2 shows the effect of Pd loading on the catalytic properties of Pd/SnO_2 and $Pd/TiO_2–SnO_2$ for nitrate reduction. The catalytic activity and selectivity of the $Pd/TiO_2–SnO_2$ catalysts were superior to those of Pd/SnO_2 under the same Pd loading. The Pd loading has significant effects on the catalytic performances of Pd/SnO_2 and $Pd/TiO_2–SnO_2$ in a nitrate reduction system. The catalytic activity of $Pd/TiO_2–SnO_2$ was positively related to the Pd load ratio, but the ascending function decreased when the Pd load ratio was more than 4% because the few metal active sites and low Pd loading can result in a slow reaction rate of the catalytic reduction. Thus, the catalytic activity increases as a result of the increased Pd atomic number on the surface of the unit quantity catalyst. The catalytic reduction of nitrate is a heterogeneous catalytic process in which only the metal atoms on the surface have catalytic activity. Continuously increasing Pd loading may cause the conglomeration of Pd particles; hence, the catalytic activity is not significantly enhanced when the Pd loading is over 4%.

The catalytic selectivity of $Pd/TiO_2–SnO_2$ was negatively related to the Pd load ratio primarily because the main factors that control NH_4^+ formation are related to active H availability and NO/N surface coverage would appear [1,23]. Active H generated by hydrogen spill-over increases as the Pd loading increases, and NH_4^+ will be formed when NO/N collides with excess H since the relative surface concentration of NO and N are low compared to active H.

Therefore, a Pd load ratio of 4% is suitable for efficient nitrate reduction.

3.4. Influence of different formic acid concentrations on $Pd/TiO_2–SnO_2$ catalytic properties after TiO_2 doping

Catalytic experiments were performed using 10% TiO_2 mol fraction, 4% Pd loading and 4.0–16.0 mmol/L formic acid. Table 3 shows that the catalytic activity and selectivity of $Pd/TiO_2–SnO_2$ are superior to those of Pd/SnO_2 using the same formic acid concentration. However, the concentration of NH_4^+ is still higher than the admissible level. The amount of formic acid has significant effects on the catalytic performances of Pd/SnO_2 and $Pd/TiO_2–SnO_2$ in a nitrate reduction system. The catalytic activity of $Pd/TiO_2–SnO_2$ is positively related to the amount of formic acid, with less formic acid resulting in a low nitrate removal rate and low catalytic activity. As the formic acid amount increases, the nitrate removal efficiency and the catalytic activity increase rapidly, but the catalytic selectivity gradually decreases because excessive hydrogen produced

Table 2
The effect of Pd on the catalytic properties for nitrate reduction.

Pd loading	Degradation (%)		Activity (mg/(min g_{cata}))		NH_4^+ concentration (mg/L)	
	Pd/SnO_2	Pd/TiO_2–SnO_2	Pd/SnO_2	Pd/TiO_2–SnO_2	Pd/SnO_2	Pd/TiO_2–SnO_2
2	45.0	70.1	0.98	1.97	5.9	2.4
3	65.4	85.3	1.42	2.99	8.9	3.8
4	95.8	100	2.08	4.00	13.0	5.2
5	100	100.0	2.11	4.08	14.5	6.8
6	100	100.0	2.20	4.18	15.3	8.3.

by formic acid decomposition will hydrogenate NO and form a by-product of NH_4^+. The basic reactions of formic acid and nitrate are as follows [24]:

$$2NO_3^- + 5HCOOH \rightarrow N_2 + 3CO_2 + 2HCO_3^- + 4H_2O \quad (1)$$

$$NO_3^- + 4HCOOH \rightarrow NH_4^+ + 2CO_2 + 2HCO_3^- + H_2O \quad (2)$$

Theoretically, approximately 4.0 mmol/L of formic acid will be consumed for the transformation of 100 mg/L of nitrate. However, the extent of nitrate conversion of Pd/SnO_2 and Pd/TiO_2–SnO_2 are merely 40.6% and 54.0%, respectively. This phenomenon may be due in part to the formic acid decomposition hydrogen being consumed by the precious metal palladium hydrogen spillover effect [25]. The results also show that a complete conversion of nitrate, a high activity and a low amount of NH_4^+ is obtained when the formic acid concentration is 1.6 mmol/L and a complete mineralization of formic acid is only obtained when its formic acid concentration is lower than 1.6 mmol/L.

3.5. Stability of Pd/TiO_2–SnO_2

The initial pH value using formic acid as the reducing agent in acidic environments is approximately 3–4 in the catalytic reduction system. However, noble metals may display dissolution phenomena under acidic conditions; thus, the acidic stability of these catalysts in water needs to be determined. The residual ions in the solution after the reaction were detected using ICP-OES. The results showed that the dissolved Pd ions were not detected in the catalytic reduction system using Pd/SnO_2 or Pd/TiO_2–SnO_2 as the catalyst, indicating that the catalyst was stable under acidic conditions. Yoshinaga et al. discovered that the dual-metal catalysts using γ-Al_2O_3, SiO_2 and ZrO_2 as the carrier apparently dissolved under acidic conditions, while the activated carbon carriers were more stable and had no metal dissolution, illustrating that the acidic stability of mono/bimetallic catalysts differed depending on the carriers used [26].

The catalysts were washed several times, centrifuged and then dried at room temperature and recycled to evaluate the long-term stability of the catalyst with the same amount of nitrate and formic acid after 90 min nitrate reduction in water. The experimental results are summarized in Table 4. The activity and selectivity of Pd/TiO_2–SnO_2 did not decline after reusing them 5 times, but the activity and selectivity of Pd/SnO_2 was decreased by 30%. These results illustrated that Pd/TiO_2–SnO_2 has much better stability than Pd/SnO_2 and can meet the challenge of repeated use.

4. The reaction mechanism of catalytic reduction

XPS analysis was conducted to confirm the oxidation state of the palladium (Fig. 5), tin (Fig. 6) and titanium (Fig. 7) species. In Fig. 5, the peaks at 335.7 eV (335.4 eV) and 340.5 eV (340.3 eV) are assigned to Pd $3d_{5/2}$ and Pd $3d_{3/2}$, respectively, indicating that palladium was present on the catalyst surface in its metallic form. The comparison between Fig. 5(a) and (b) shows that the position of the Pd $3d_{5/2}$ peak shifted from 335.7 eV to 335.4 eV after TiO_2 doping. The negative displacement occurred because of the change in the chemical environment and the energy state of the Pd components due to the accelerated electron transfer between Pd and the carrier leads changing the Pd binding energy. Meanwhile, tin was found in both its bivalent Sn and quadrivalent Sn forms (Fig. 6). The Sn 3*d* spectrum contains a double peak with binding energies of 486.3 (485.8) eV and 494.7 (494.2) eV, which can be assigned as Sn $3d_{5/2}$ and Sn $3d_{3/2}$ lines, respectively. Discrimination between SnO and SnO_2 in photoemission studies is complicated because of the very small shift in Sn 3*d* core level binding energies for different tin oxide compositions [27]. The binding energies of Sn $3d_{5/2}$ for SnO and SnO_2 almost mix with each other, as shown by measurements using different XPS instruments [28]. The key to understanding the many aspects of the tin oxide surface properties is the dual valence of the Sn ions. To better understand the surface composition of the oxide, its O/Sn ratio was calculated according to Wu et al., giving a value of 1.52 [29], which indicated that the tin oxide in the catalysts was of high oxygen vacancy. The peak (Fig. 7) located at 457.2 eV was attributed to trivalent titanium, while the peak at 462.7 eV was assigned to TiO_2. The wider peak area of Ti $2p_{3/2}$ (457.4 eV) revealed that titanium mainly existed in the form of trivalent titanium. Ti_2O_3 is non-stoichiometric, which indicates many oxygen

Table 3
The effect of formic acid concentration on the catalytic properties for nitrate reduction.

Formic acid concentration (mmol/L)	Degradation (%)		Activity (mg/(min g_{cata}))		NH_4^+ concentration (mg/L)		Conversion of formic acid (%)
	Pd/SnO_2	Pd/TiO_2–SnO_2	Pd/SnO_2	Pd/TiO_2–SnO_2	Pd/SnO_2	Pd/TiO_2–SnO_2	Pd/TiO_2–SnO_2
4.0	40.6	54.0	0.70	1.20	4.9	2.3	100
8.0	58.0	89.5	1.10	1.98	6.8	3.1	100
12.0	88.1	95.4	1.70	2.32	7.5	4.5	100
16.0	95.8	100.0	2.08	4.00	13.0	5.2	100
20.0	100	100.0	2.60	4.06	15.7	8.0	86.3
24.0	100	100.0	2.70	4.23	19.1	11.6	56.8

Table 4
The catalytic results for reused Pd/SnO_2 and Pd/TiO_2–SnO_2 catalysts.

Reused time	Degradation (%)		Activity (mg/(min g_{cata}))		NH_4^+ concentration (mg/L)	
	Pd/SnO_2	Pd/TiO_2–SnO_2	Pd/SnO_2	Pd/TiO_2–SnO_2	Pd/SnO_2	Pd/TiO_2–SnO_2
1	95.8	100	2.08	4.00	13.0	5.2
2	85.0	99.5	1.89	3.89	10.5	5.4
3	75.9	99.7	1.70	3.92	9.14	5.9
4	70.7	99.8	1.50	3.90	8.26	5.5
5	65.1	99.4	1.25	3.85	7.04	4.6

Table 5
XPS data of different chemical states of O and Sn and Ti elements on the surface of Pd/SnO_2 and Pd/TiO_2–SnO_2.

Samples	Atomic number ratio of O_L and Sn and Ti	Percentage of O_L	Percentage of O_{-OH}	Percentage of O_S	Evaluated percentage of oxygen vacancies
Pd/SnO_2	100:56.8	75.4	16.9	7.7	13.6
Pd/TiO_2–SnO_2	100:58.5:4.2	70.1	29.0	0.90	25.4

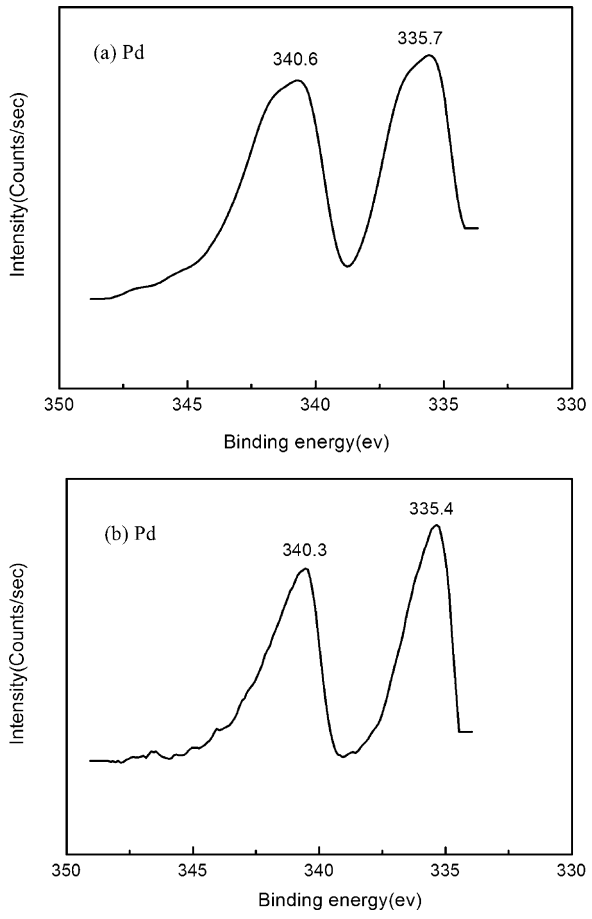

Fig. 5. X-ray photoelectron spectroscopy images of Pd in catalysts (a) Pd/SnO_2 and (b) Pd/TiO_2–SnO_2.

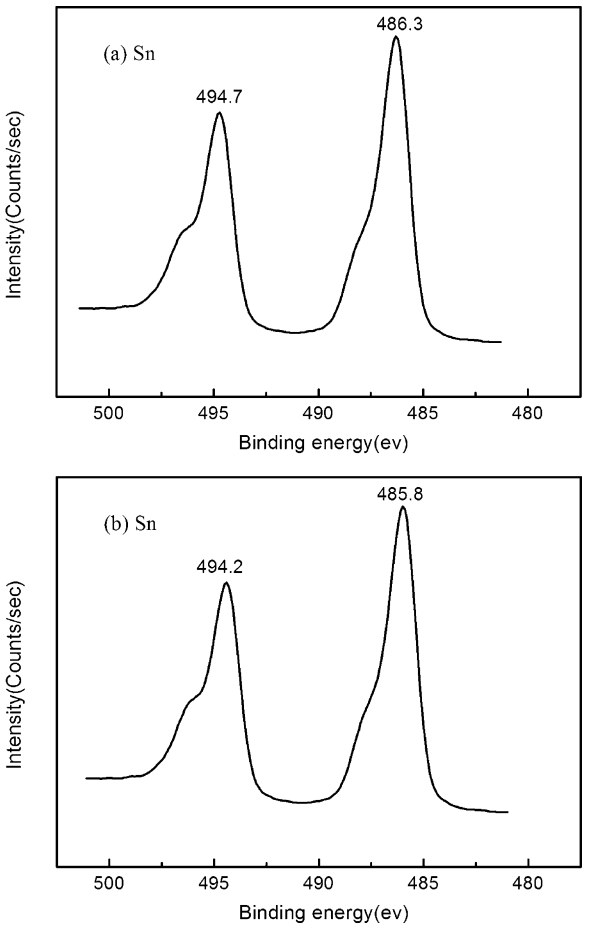

Fig. 6. X-ray photoelectron spectroscopy images of Sn in catalysts (a) Pd/SnO_2 and (b) Pd/TiO_2–SnO_2.

vacancies. The approximate formulas for calculating the percentage of oxygen vacancies are as follows:

$$V_O\,\% = \frac{((\text{The atomic number ratio of Ti and Sn}) \times 4) - (\text{The atomic number ratio of } O_L \times 2)}{2} \times 100$$

Table 5 shows the XPS data of O and Sn and Ti elements on the surface of Pd/SnO_2 and Pd/TiO_2–SnO_2, where V_O is the oxygen vacancy, O_L is the lattice oxygen, O_{-OH} is the surface hydroxyl oxygen and O_S is adsorbed oxygen. Based on the data of Table 5, it can be found that the amount of oxygen vacancy of Pd/TiO_2–SnO_2 increased. Gavagnin et al. suggested that the role of SnO_x could be very important in promoting the activity and selectivity of the catalysts because of some oxygen vacancies created on SnO_2 by hydrogen spill-over from the Pd metal [16]. More emerging oxygen vacancies form more catalytic activity centers after TiO_2 doping,

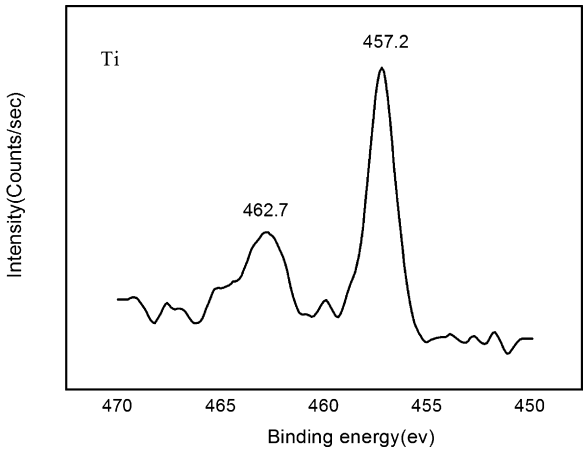

Fig. 7. X-ray photoelectron spectroscopy images of Ti in catalyst $Pd/TiO_2–SnO_2$.

illustrating that $Pd/TiO_2–SnO_2$ has better catalytic properties than Pd/SnO_2.

5. Conclusions

A monometallic catalyst, $Pd/TiO_2–SnO_2$, was prepared using the co-precipitation method by impregnating Pd on the surface of a composite support of $TiO_2–SnO_2$. The TiO_2 hindered the SnO_2 nucleation process of conglomeration. The smallest particle size was obtained using 10% TiO_2 mol fraction, with a size of 9.1 nm and a maximum specific surface area of 100.08 m^2/g.

The best catalytic properties of the formic acid–$Pd/TiO_2–SnO_2$ system were obtained using a mol fraction of 10% TiO_2. The catalytic activity increased from 2.08 mg/(min g_{cata}) of Pd/SnO_2 to 4.00 mg/(min g_{cata}) of $Pd/TiO_2–SnO_2$, while the NH_4^+ concentration decreased from 13.0 mg/L to 5.2 mg/L, demonstrating that the catalytic activity and selectivity were both improved after TiO_2 doping. No dissolved Pd ions were detected in the catalytic reduction system regardless of the catalyst used, Pd/SnO_2 or $Pd/TiO_2–SnO_2$, indicating that both of the catalysts had good stability under acidic conditions. $Pd/TiO_2–SnO_2$ remained active and selective after reusing it many times, but the activity and selectivity of the reused Pd/SnO_2 decreased by 30%.

The results of the XPS analysis of Pd/SnO_2 and $Pd/TiO_2–SnO_2$ indicated that both of the catalysts were of high oxygen vacancy. $Pd/TiO_2–SnO_2$ has better catalytic properties than Pd/SnO_2 may attribute to the increased amount of oxygen vacancy by TiO_2 doping.

Acknowledgement

The authors gratefully acknowledge the financial support provided by the National S&T Major Project Foundation of China (No. 2008ZX07211-005).

References

[1] J. Sá, J. Montero, E. Duncan, J.A. Anderson, Applied Catalysis B 73 (2007) 98.
[2] D.M. Freedman, K.P. Cantor, M.H. Ward, K.J. Helzlsouer, Archives of Environment Health 55 (2000) 326.
[3] Y. Wang, J.H. Qu, H.J. Liu, Journal of Molecular Catalysis A: Chemical 272 (2007) 31.
[4] K.D. Vorlop, T. Tacke, M. Eur, Patent DE3830850 A1 (1998).
[5] W.L. Gao, N.J. Guan, J.X. Chen, X.X. Guan, R.C. Jin, H.S. Zheng, Z.G. Liu, F.X. Zhang, Applied Catalysis B 46 (2003) 341.
[6] A. Pintar, J. Batista a, I. Muševič, Applied Catalysis B 52 (2003) 49.
[7] Z.Y. Xu, L.Q. Chen, Y. Shao, D.Q. Yin, S.R. Zheng, Industrial and Engineering Chemistry Research 48 (2009) 8356.
[8] D.J. Wan, H.J. Liu, X. Zhao, J.H. Qu, S.H. Xiao, Y.N. Hou, Journal of Colloid and Interface Science 332 (2009) 151.
[9] B.P. Chaplin, J.R. Shapley, C.J. Werth, Catalysis Letters 130 (2009) 56.
[10] S. Horold, K.D. Vorlop, T. Tacke, M. Sell, Catalysis Today 17 (1993) 21.
[11] U. Prüsse, K.D. Vorlop, Journal of Molecular Catalysis A: Chemical 173 (2001) 313.
[12] K. Nakamura, Y. Yoshida, I. Mikami, T. Okuhara, Applied Catalysis B 65 (2006) 31.
[13] O.S.G.P. Soares, J.J.M. Órfão, M.F.R. Pereira, Applied Catalysis B 91 (2009) 441.
[14] J. Sá, T. Berger, K. Föttinger, A. Riss, J.A. Anderson, H. Vinek, Journal of Catalysis 234 (2005) 282.
[15] F. Epron, F. Gauthard, J. Barbier, Journal of Catalysis 206 (2002) 36.
[16] R. Gavagnin, L. Biasetto, F. Pinna, G. Strukul, Applied Catalysis B 38 (2002) 91.
[17] Z.Q. Liu, J. Ma, Z.L. Zhang, J.F. Liang, X.Y. Yang, Chinese Journal of Catalysis 25 (2004) 302.
[18] C.S. Mei, S.H. Zhong, Chinese Journal of Chemical Physics 18 (2005) 821.
[19] Z.L. Xu, B.Y. Xue, Q.J. Yang, C. Xie, J.B. Zhang, Y.G. Du, Chinese Journal of Applied Chemistry 21 (2004) 980.
[20] U. Prusse, M. Kroger, K.D. Vorlop, Chemie Ingenieur Technik 69 (1997) 87.
[21] N. Barrabés, A. Dafinov, F. Medina, J.E. Sueiras, Catalysis Today 149 (2010) 341.
[22] X. Fu, L.A. Clark, Q. Yang, Environmental Science and Technology 30 (1996) 647.
[23] Y.X. Chen, Y. Zhang, G.H. Chen, Water Research 37 (2003) 2489.
[24] A. Garron, F. Epron, Water Research 39 (2005) 3073.
[25] A. Pintar, M. Setinc, J. Levec, Journal of Catalysis 174 (1998) 72.
[26] Y. Yoshinaga, T. Akita, I. Mikami, T. Okuhara, Journal of Catalysis 207 (2002) 37.
[27] G. Gaggiotti, A. Galdikas, S. Kaciulis, G. Mattogno, A. Setkus, Journal of Applied Physics 76 (1994) 4467.
[28] T. Schneider, M. Sommer, J. Goschnick, Applied Surface Science 252 (2005) 257.
[29] Q.H. Wu, J. Song, J.C. Li, Surface and Interface Analysis 40 (2008) 1488.